Coupling and coordinated development relationship between ecological environment and carbon emission in Chinese counties

Qi Tang, Li Hua*, Jieling Tang, Long Jiang, Qian Wang, Yunfei Cao and Chongfa Cai

College of Resources and Environment, Huazhong Agricultural University, Wuhan , 430070, China

Abstract

The coupling and coordinated relationship between the ecological environment and carbon emissions is critical to the sustained development of human society. The remote sensing eco-index (RSEI) model has been applied to the assessment and monitoring of ecological environment quality, but RSEI neglects air pollution, and thus this study introduced aerosol optical depth (AOD) into the index system and constructed a novel ARSEI to evaluate the ecological environment quality and analyze the spatial-temporal changes in ARSEI and energy-related carbon emission (ECE) at the county level in China. Additionally, we further investigate the local relationship between ARSEI and ECE in China by using the coupled coordination model (CCD). The outcomes showed that: (1) Compared with the RSEI, the ARSEI widened the gap in ecological quality between the east and the west along the Heihe-Tengchong line; (2) ARSEI value was significantly increased in 24.70% of areas in China, mainly in the Northeast Plain, Loess Plateau, and Tarim Basin. ARSEI value was significantly decreased in 5.35% of areas in China, mainly in the Qinghai-Tibetan Plateau, the northern part of the Tianshan Mountains, eastern coastal cities, and central urban agglomerations; (3) ECE dispersed from east to the west from 2000 to 2017, with an average annual increase of > 0.3 megatons in 354 counties, densely distributed in the eastern coastal urban agglomerations, Loess Plateau, and sporadically distributed in some central and western cities in China; (4) CCD distribution showed a "west-low-east-high" pattern, with an upward trend in CCD value in the majority of surveyed counties (2,241), and a downward trend in some counties (171) in southwest, south, and central China. Based on these results, recommendations are proposed at the county and above levels for coordinated and sustainable development of urban economy and ecology.

Keywords : ARSEI ; CCD; Ecological restoration ; Economic development ; Spatiotemporal variation

1. Introduction

Climate change and anthropogenic interference activities pose a major challenge to the environment and people around the world (Custer and Dini-Andreote, 2022). Carbon emissions, mainly from fossil fuel combustion, affect the natural environment of the earth's surface (Wise et al., 2009), exacerbate global warming, increase the frequency of extreme weather, and even lead to continuous ecological deterioration such as land degradation, air pollution, and desertification (Liu et al., 2022; Liu et al., 2019). Since 2006, China has become the world's largest producer of carbon dioxide due to its rapid economic development (Teng, 2015), accounting for one-third of the global total by 2021 (IEA, 2021). Fortunately, China has been committed to the construction of emission reduction, and the emission reduction speed is an important factor in limiting global warming to 1.5ºC. The ecological environment can interact with carbon emissions(An et al., 2023a; Chen et al., 2020b) and a good ecological environment can bear more carbon emissions (Lv et al., 2019). Quantifying the relationship between the ecological environment and carbon emissions will promote the sustained development of human society.

Remote sensing technology overcomes the limitation of data collection and analysis scale, and the cloud computing platform (Such as Google Earth Engine) makes large-scale ecological quality monitoring possible (Jin and Shi, 2022; Liu et al., 2023). Remote sensing eco-index (RSEI) model proposed by Xu (Yu et al., 2022b) in 2013 can quickly and objectively evaluate the ecological quality

* Corresponding author. Tel.:13871545328.

E-mail address: huali@mail.hzau.edu.cn.

status of a large region by integrating multiple ecological indicators through principal component analysis (PCA), and RSEI has been successfully applied to many countries and regions (Fan et al., 2020; Yang et al., 2022; Ye, 2022; Zhang et al., 2022a). The RSEI model indicators include normalized difference vegetation index (NDVI), humidity (WET), land surface temperature (LST), normalized difference bare soil index (NDBSI), but in RSEI model, only natural environmental conditions on the earth surface are taken into consideration, with the air pollution problems caused by dense population and industrial production neglected (He et al., 2017), and the assessment of urban air quality is lacking in this model. The carbon emission in this study refers to energy-related carbon emission (ECE), accounting for 88% of total carbon emission in China in 2021, bringing about a series of pollution problems and increasing human health risks. In this study, we introduced aerosol optical depth (AOD) index(Xin et al., 2023; Yang et al., 2021), which is highly related with air pollution, into the RSEI model, thus forming a novel remote sensing ecological index (ARSEI).

Coupling impacts refers to the interaction between two or more systems (Lenzen et al., 2016). Ecological environment and carbon emissions can interact, and thus they have coupling effects. Specifically, large amounts of carbon emissions can pose threats to the natural environment and human society, such as the pollution of the atmosphere, soil, and water resources, and the heat island effect. However, good vegetation conditions can absorb CO_2 in the air, and slow and control the rise of CO_2 and temperature to some extent (Le Quere et al., 2018). Land use and urban planning (such as planning of the river network, transportation, and housing) will affect population density and industrial layout. The direct interaction between the ecological environment and carbon emission in the region is known as the local coupling of the two. The coupling coordination degree model (CCD) has been widely used to evaluate the coupled impacts between urbanization and the ecological system (Cai et al., 2021; Tang et al., 2022; Wang et al., 2019) and to investigate the coupling relationship between social factors and ecological environment (Fan et al., 2019), but the studies on the local coupled impacts between carbon emission and ecological environment need to be further conducted to provide directional carbon emission reduction measures for the region development. Currently, the main related research is performed at the provincial and municipal levels (An et al., 2023a; Chen et al., 2020b). However, China's investment and financial subsidies in ecological protection are at the county level (Huang et al., 2018). Therefore, this study referred to the research on county-level energy-related carbon emission (ECE) by Chen et al. (Chen et al., 2020a), which can further evaluate the development of carbon emissions from the county-level and regional city perspectives, and the CCD model provides insights into local coupling between ECE and ARSEI.

Therefore, in this study, we constructed an ARSEI model to evaluate China's ecological environmental quality from 2000 to 2022 and analyze its spatial-temporal change characteristics. We used the CCD model to reveal the coupling and coordinated development relationship between ARSEI and county-level carbon emissions and their trends in China from 2000 to 2017. The main objectives of this research are to (1) improve RSEI model by introducing aerosol (AOD) so as to realize the assessment of China's ecological environment quality at the pixel scale, and (2) to compute CCD values between ARSEI and ECE based on the concept of localized coupling. Finally, this study provides decision-making basis for the regional environmental protection, the coordinated sustainable development of the city, and the governance of the country.

2. Materials and methods

2.1. Study area

The Heihe-Tengchong line divides China into two different geographical regions (east and west). The west is high in terrain and small in population, while the east is low in terrain and large in population, and the east better developed economically than the west. Figure 1 shows that China is divided into six geographic regions, namely, northeast, northwest, north, east, southwest, and central-south.

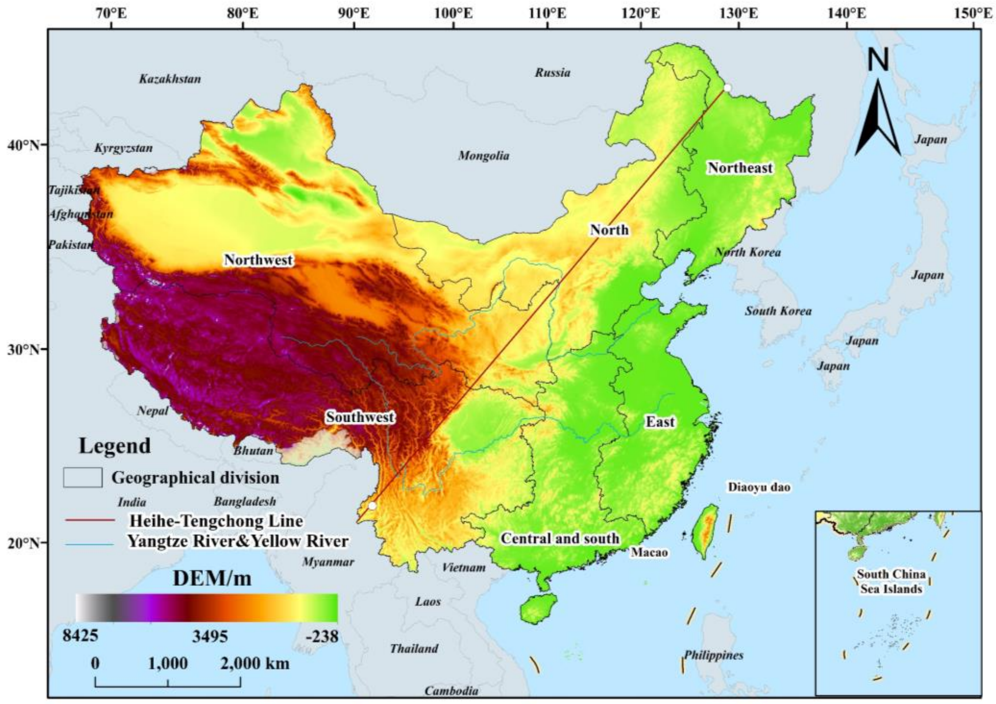

Fig. 1. Location of the study area

2.2. Data preparation and preprocessing

The novel remotely sensed ecological index ARSEI model constructed in this study involved five components, namely, normalized difference vegetation index (NDVI), humidity (WET), land surface temperature (LST), normalized difference bare soil index (NDBSI), and aerosol optical depth (AOD). In order to minimize the disturbance due to the inconsistency of imagery collection time, we acquired four remote sensing image datasets (MOD09A1, MOD11A2, MOD13A1, and MCD19A2) in the 2000-2022 growing seasons (July-September) from the GEE platform (Long et al., 2023). In this study, dataset MOD09A1 was used to calculate WET and NDBSI. Dataset MOD11A2 daytime band with better data quality was used to obtain LST. Dataset MOD13A1 was employed to provide NDVI. Dataset MCD19A2 provided AOD. The corrected normalized water index (MNDWI) was used for water removal in the research area. In addition, we de-clouded the ground reflectance data based on MODIS quality control (QC) files to eliminate low-quality pixels so as to improve the image quality (Xu and Shen, 2013), and used median synthesis to improve the data reconstruction performance. The county-level energy-related carbon emission data (NCE) were derived from the research by (Chen et al., 2020a) with data accuracy of up to > 95%. The county-level carbon emission data were collected from 2000 to 2017. The temporal and spatial resolutions of each data source are listed in Table 1.

Table1. Data sources

Data	Spatial resolution	Temporal resolution	Time range	Data sources
MOD09A1	500m	8d	2000-2022 growing season (July-September)	Google Earth Engine
MOD11A2	1000m	8d	2000-2022 growing season (July-September)	Google Earth Engine
MOD13A1	500m	16d	2000-2022 growing season (July-September)	Google Earth Engine
MCD19A2	1000m	1d	2000-2022 growing season (July-September)	Google Earth Engine
Carbon Emissions Data	County	Year	2000-2017	https://doi.org/10.6084/m9.figshare.c.5136302.v2
Land Use Data	30m	year	2000-2021	https://doi.org/10.5281/zenodo.4417810
Meteorological Data	—	day	2000-2021	National Meteorological Service
Statistics	—	—	2000-2021	Ecological Bulletin

2.3. Calculation of ARSEI values

RSEI model is constructed based on four indexes (NDVI, WET, NDBSI, and LST) that are closely related to the ecological environment and human activities (Hu and Xu, 2018), and the RSEI model data are easily accessible and currently widely used in the research on ecological environment evaluation (Aizizi et al., 2023; Xiong et al., 2021; Yang et al., 2023). We introduced the AOD index into RSEI to construct the ARSEI model (Zhang et al., 2023a). The calculation formula for each index is shown in Table 2.

Table2. Calculation formulae for NDVI, WET, LST, NDBSI, and MNDWI.

Indicator	Formula	Details
NDVI	$(B_{nir} - B_{red})/(B_{nir} + B_{red})$	B_{nir} and B_{red} represent near infrared bands (NIR) and red bands in MOD13A1dataset.
WET	$0.1147\,B_{red} + 0.2489\,B_{nir1} + 0.2408B_{blue} + 0.3132B_{green} - 0.3122B_{nir2} - 0.6416B_{sr1} - 0.5087B_{sr2}$	B_{red}, B_{blue}, B_{green}, B_{nir1}, B_{nir2}, B_{sr1}, and B_{sr2} represent red, blue, green, NIR1, NIR2, shortwave IR1, shortwave IR2 bands in MOD09A1 dataset, respectively
LST	$0.02B_1 - 273.15$	B_1represents the LST band in the MOD11A2 dataset
NDBSI	SI=$\frac{(B_{sr1}+B_{red})-(B_{blue}+B_{nir})}{(B_{sr1}+B_{red})+(B_{blue}+B_{nir})}$ IBI=$\frac{2B_{sr1}(B_{sr1}+B_{nir})-[\frac{B_{nir}}{(B_{red}+B_{nir})}+\frac{B_{green}}{(B_{sr1}+B_{green})}]}{2B_{sr1}(B_{sr1}+B_{nir})+[\frac{B_{nir}}{(B_{red}+B_{nir})}+\frac{B_{green}}{(B_{sr1}+B_{green})}]}$ NDBSI=(SI+IBI)/2	SI and IBI represent soil index and index-based built-up index, respectively
MNDWI	$(B_{green} - B_{swir1})/(B_{green} + B_{swir1})$	B_{green} and B_{swir1} represent green band and shortwave IR1 band in MOD09A1dataset, respectively.
AOD	Optical_Depth_047 band of the MCD19A2 product	

$$ARSEI_0 = f(NDVI\ , WET, NDBSI, LST, AOD) \quad (1)$$

$$ARSEI = \frac{ARSEI_0 - ARSEI_{0min}}{ARSEI_{0max} - ARSEI_{0min}} \quad (2)$$

Due to the inconsistency of the dimensions of the five indexes, the normalization processing was performed before the principal component analysis, and these indexes were resampled to unify the spatial resolution (1000m). $ARSEI_0$ is the first primary component of the five indexes, and f is the normalization processing of the five indexes. The ARSEI was obtained by normalizing $ARSEI_0$. The range of the final ARSEI value was between 0 and 1. The closer to 1 the ARSEI, the higher the ecological environment quality. The ARSEI was categorized into five levels including Level 1 (Poor), 0-0.2; Level 2 (Fair), 0.2-0.4; Level 3 (Moderate), 0.4-0.6; Level 4 (Good), 0.6-0.8 and Level 5 (Excellent), 0.8-1.0 (Xiong et al., 2021).

2.4. Trend analysis

The temporal and spatial distribution and variation characteristics of the ecological environment quality in China from 2000 to 2022 were analyzed by Theil-Sen median trend method combined with Mann-Kendall (MK) test. This method was more robust than the traditional linear regression method since it could avoid the interference of outliers, and thus it has been widely used in the time-series analysis of data. The calculation method of Theil-Sen value (β) was as follows:

$$\beta = Median\frac{ARSEI_j - ARSEI_i}{j-i}, 2000 \le i \le j \le 2022 \tag{3}$$

Where i and j are the time series years of ARSEI; and $ARSEI_i$ and $ARSEI_j$ denote the ARSEI value in the i^{th} year and the j^{th} year, respectively.

The MK test used Z-value for significance test with a significance level of α. ARSEI variation at time series was considered as significant when $|Z|>Z_{1-\alpha/2}$. In this study, α was set as 0.05, indicating that the time series was significant at the 95% confidence level, the corresponding Z value in the formula was 1.96 (Tang et al., 2023). Referring to the research by Long et al. (Long et al., 2023), we combined the Theil-Sen median and Z-value were used to categorize ARSEI trends into five classifications, as shown in Table 3.

Table3 Classification criteria for ARSEI change trends

Classification criteria	ARSEI change trends
$\beta < -0.0005$ and $|Z| > 1.96$	Significant degradation
$\beta < -0.0005$ and $|Z| \le 1.96$	Slight degradation
$-0.0005 \le \beta \le 0.0005$	Basically stable
$\beta > 0.0005$ and $|Z| \le 1.96$	Slight improvement
$\beta > 0.0005$ and $|Z| > 1.96$	Significant improvement

2.5 Spatial autocorrelation analysis

Spatial autocorrelation analysis is to study the correlation of the same attributes which are very close. In this study, Moran's I index (Getis and Ord, 1992) and Lisa index (An et al., 2023b) were used to show the spatial autocorrelation between ARSEI and ECE. Moran's I index ranges from -1 to 1, with Moran's I < 0 denoting a negative correlation, Moran's I = 0 representing an uncorrelation, and Moran's I > 0 denoting a positive correlation. The Lisa index represented different aggregation patterns within the same region, including four types: LL (low-low aggregation), HH (high-high aggregation), HL (low value aggregation around high values), and LH (high value aggregation around low-values) types.

2.6 CCD model

We used the CCD model to explore the local coupling relationship between ARSEI and energy-related carbon emission (ECE) in China. The CCD model was expressed in formula as below:

$$C = \left\{\frac{U \times E}{[(U+E)/2]^2}\right\}^{\frac{1}{2}} \tag{4}$$

Where C is the coupling degree between ARSEI and ECE, the value of C is in the range of 0-1, U is ECE, and E is ARSEI.

In order to avoid the problem of "false coordination", that is, U and E are low, C is high on the contrary, the CCD model is improved to consider the coupling degree. (Xu et al., 2021):

$$D = \sqrt{C \times \mathrm{T}} \tag{5}$$

$$\mathrm{T} = \alpha U + \beta E \tag{6}$$

Where D represents the degree of coordination between the two systems; T represents the contribution of both systems. Since U and E are equally important in this study, it is set to 0.5. To further analyze the level of coupling coordination between ARSEI and ECE, we divided their CCD values into five categories：severe incoordination (0-0.2)，(0.2-0.4) slight incoordination，(0.4-0.6) bare coordination，(0.6-0.8) slight coordination，(0.8-1) high coordination.

3. Results

3.1 Ecological environment quality in China

3.1.1 Rationality analysis of ARSEI model

The principal component (PCA) analysis results of the five indexes of ARSEI model from 2000 to 2022 showed that the eigenvalue contribution of the PCA1 was as high as 87.11% (in 2015), and as low as 83.57% (in 2020) (Table 4). The multi-year average contribution of PCA1 was above 80%, indicating that PCA1 concentrated the five ecological index information to the largest degree. In PCA1, the characteristic loads NDVI and WET are positive, while LST, NDBSI and AOD are negative, which accords with the actual situation, indicating that PCA1 provided a reasonable interpretation of each ecological index. Therefore, it was reasonable to construct ARSEI model based on PCA1 to estimate the ecological environment quality in China.

Table 4 Principal component analysis of ARSEI model

Year	Loading value of each index					Eigenvalue	PCA1 contribution(%)
	NDVI	WET	NBDSI	LST	AOD		
2000	0.6151	0.3445	-0.609	-0.3602	-0.0494	0.1939	86.89
2005	0.6369	0.3728	-0.5676	-0.351	-0.1002	0.1867	85.19
2010	0.6591	0.338	-0.5817	-0.3266	-0.0786	0.1412	85.44
2015	0.6159	0.3388	-0.6126	-0.3612	-0.0134	0.1782	87.11
2020	0.661	0.2983	-0.6214	-0.2813	-0.0939	0.1413	83.57

3.1.2 Spatial-temporal distribution of ARSEI values in China

Fig. 2 showed the spatial-temporal distribution of ARSEI values in China from 2000-2022. The Heihe-Tengchong line roughly divided China's ARSEI values into two different geographic regions (the east and the west). The overall ARSEI values in the east (ranging from 0.6 to 1.0) were higher than those in the west (ranging from 0.0 to 0.4). The areas with long-term ARSEI values ranging from 0.0 to 0.2 were mainly located in Xinjiang, Inner Mongolia, Qinghai, and Gansu Provinces, and the areas with long-term ARSEI values in the range of 0.8~1.0 were mainly concentrated in the northeast forestry region, the plains and hilly regions in central and south China and east China.

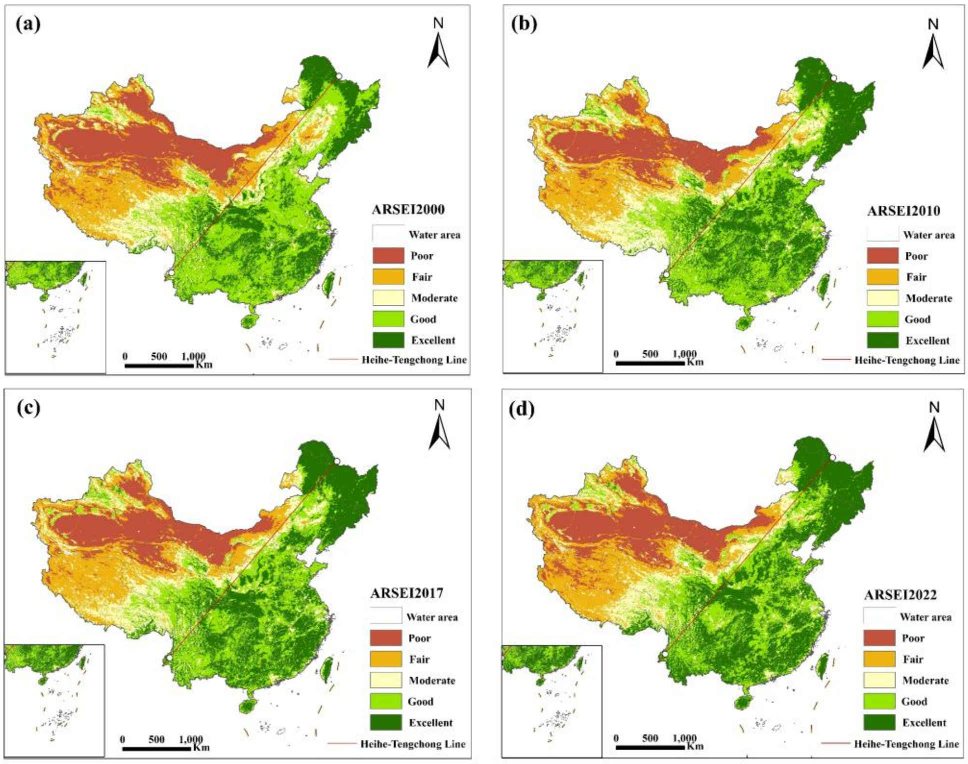

Fig. 2. Spatial distribution of the ecological environmental quality in China (ARSEI values) in 2000 (a), 2010 (b), 2017 (c), 2022 (d).

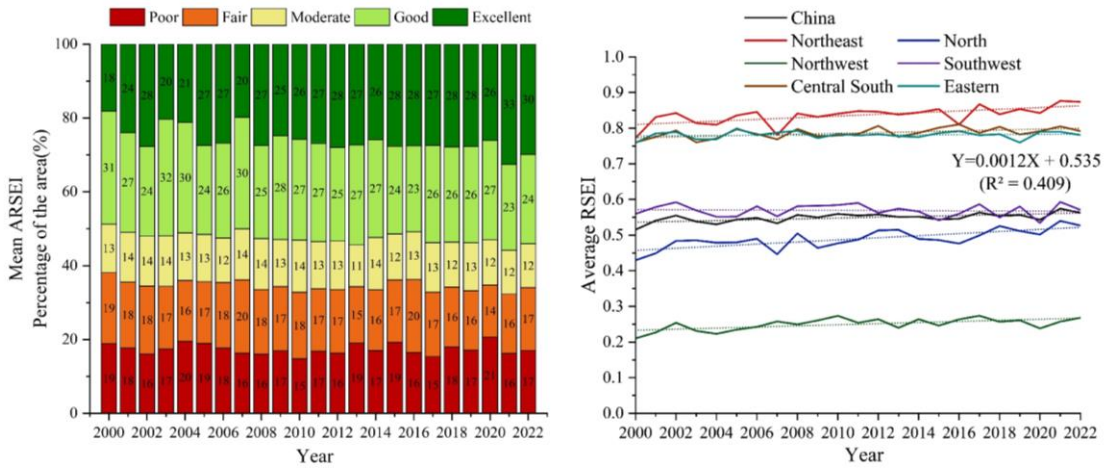

Fig. 3. Percentage of area of the regions with ARSEI levels (representing 5 different ecological qualities from poor to excellent) in China during 2000-2022 (a), and average ARSEI values in China, Northeast China, North China, Northwest China, Southwest China, South Central China, and East China (b).

3.1.3 Dynamic change trends of the ecological environment quality in China

The trend of China's ARSEI value change and the spatial distribution of its coefficient of variation (CV) was shown in Fig. 4. Table 5 showed that 24.70% of area in China exhibited a significant improvement in ARSEI value over the past 22 years, mainly distributed in North China (6.47%)and Northwest China (7.31%). Spatially, the ARSEI values of the Northeast Plain, Loess Plateau, and Tarim Basin showed a significant improvement trend. The ARSEI values of 5.35% of area in China was significantly degraded, mainly distributed in East China (1.87%) and Southwest China (1.3%). From a spatial perspective, the ARSEI values of the Qinghai-Tibet Plateau showed a significant degradation trend. In addition, the ARSEI values of some regions with faster economic development such as Beijing-Tianjin-Hebei, the Yangtze River Delta, and some urban agglomerations in central and northern China displayed a significant degradation trend. In terms of the spatial coefficient of variation, the change degree of the ARSEI value was greater in the west than in the east, and the regions with large coefficients of variation were mainly spread in Inner Mongolia, Gansu, Xinjiang, and Qinghai provinces in China.

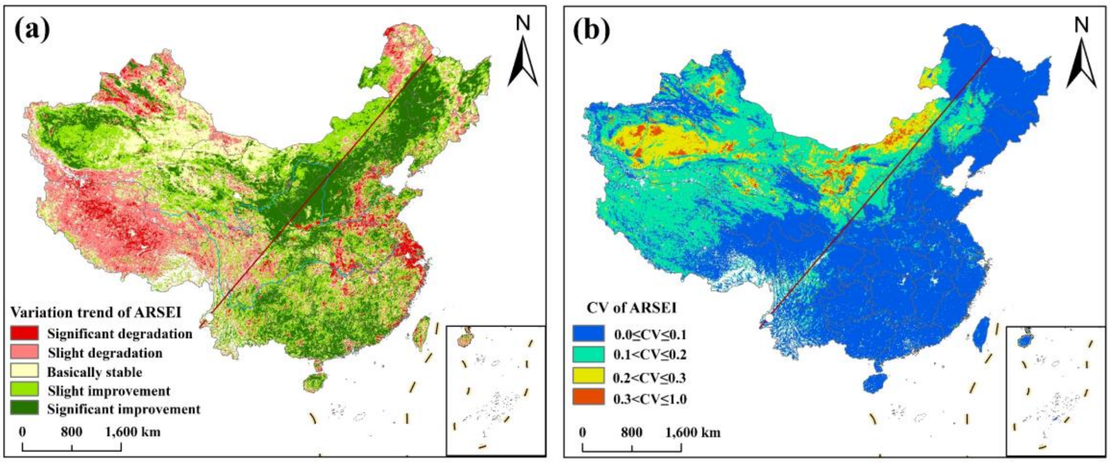

Fig. 4. Spatial distribution of ARSEI values (representing the ecological environmental quality) in China from 2000 to 2022 (a) and spatial distribution of their coefficients of variation (b).

Table5 Statistical results of ARSEI change trends in China from 2000-2022

Geographic Zoning		Northeast	North	Northwest	Southwest	Central South	Eastern	China
Significant degradation	Area(km^2)	9625	39288	80152	169629	69465	117768	485927
	Percentage(%)	0.11	0.43	0.88	1.87	0.76	1.3	5.35
Slight degradation	Area(km^2)	103647	155558	528226	866992	130209	127450	1912082
	Percentage(%)	1.14	1.71	5.81	9.54	1.43	1.4	21.03
Basically stable	Area(km^2)	157946	228515	857320	349755	135774	147652	1876962
	Percentage(%)	1.74	2.51	9.43	3.85	1.49	1.62	20.64
Slight improvement	Area(km^2)	204401	497202	793260	469418	342775	261929	2568985
	Percentage(%)	2.25	5.47	8.73	5.17	3.77	2.88	28.27
Significant improvement	Area(km^2)	309562	588080	663996	208194	314170	159683	2243685
	Percentage(%)	3.41	6.47	7.31	2.29	3.46	1.76	24.70

3.2 Spatial-temporal distribution of ECE in China

As shown in Fig. 5, the total energy carbon emissions of mainland China increased from $3.16*10^9$ tons to $9.51*10^9$ tons from 2000 to 2017, with an average annual growth of $0.44*10^9$ tons (R^2=0.93) with the overall upward trend was obvious. A faster growth rate was observed from 2000 to 2011, and the growth rate slowed down after 2011.

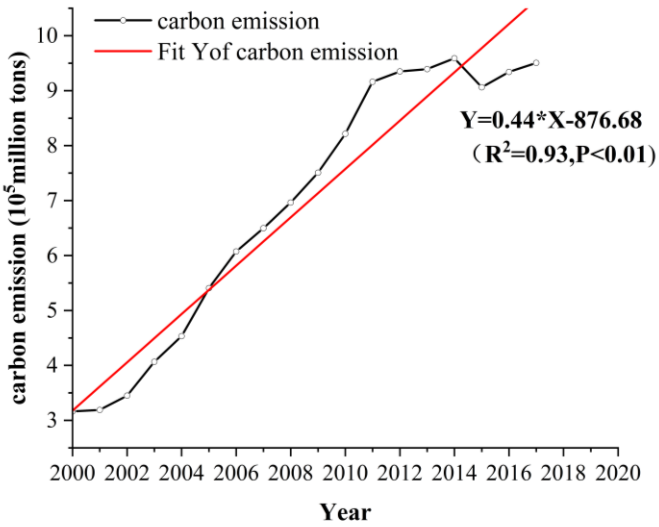

Fig. 5. Total energy-related carbon emissions (ECE) in China during 2000-2017

Fig. 6 showed that the low ECE values (0.00-1.00 million tons) were widely distributed in 2000, with 1,599 counties emitting no more than 1 megaton and 166 counties emitting more than 3 megatons, and the high ECE values (>3 million tons) were mainly spread in the eastern coastal provinces of China and in central-south China and north China, with sporadic distributions in northwest China and southwest China. In addition, overall ECE increased significantly from 2000 to 2010, with only 692 counties exhibiting low ECE and 955 counties displaying high ECE in 2010, and high-ECE areas were densely populated in the east coast, northeastern and northern regions of China. With the deepening of reform and opening up and the promotion of western development, and the acceleration of the process of urbanization, the counties with high-ECE increased spread from east to west, and the number of high-ECE counties was significantly increased in the central and western China. The increase trend of ECE slowed down from 2010 to 2017, which was consistent with the dynamics of temporal change (Fig 2). Furthermore, ECE increased in all counties in China from 2000-2017, but the degree of increase varied. From 2000 to 2017, 1239 counties exhibited an average annual increase in ECE of less than 0.1 megaton, and these counties were mainly located in the central and western parts of China. A total of 354 counties had an average annual increase of more than 0.3 megaton from 2000 to 2017, mainly densely spread in the eastern coastal areas such as the Yangtze River Delta and the Pearl River Delta as well as northern China plains, and the northeast China, Loess Plateau, western China also had scattered distribution.

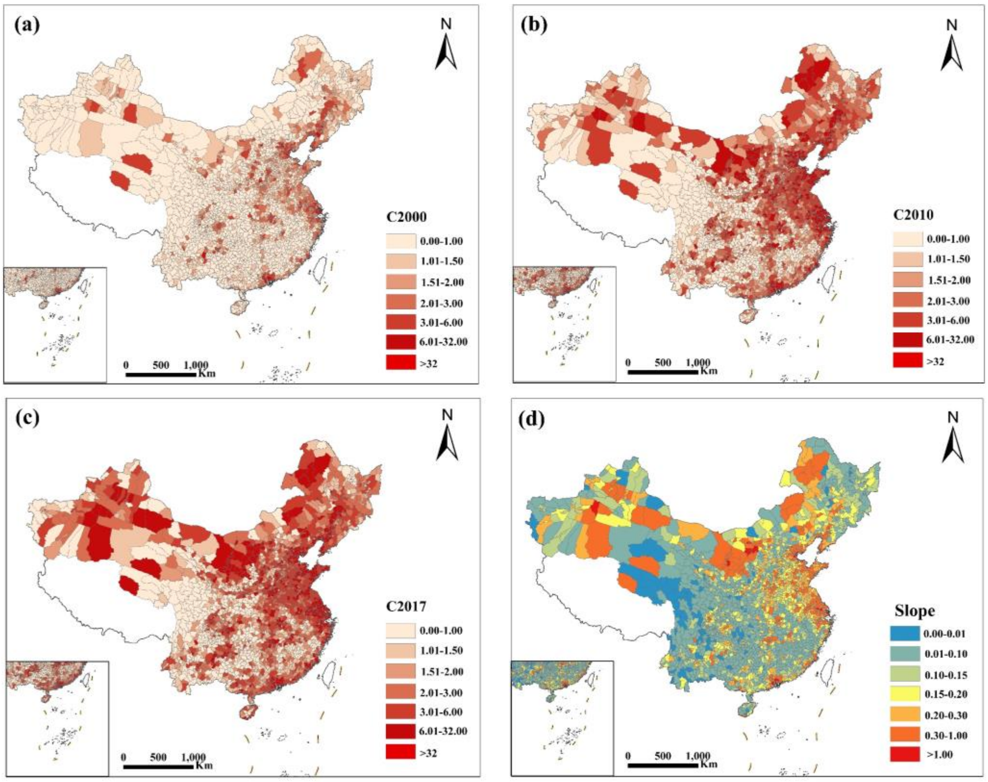

Fig. 6. China county-level energy-related carbon emissions (ECE) in 2000 (a), 2010 (b), and 2017 (c), and the carbon emission change slopes from 2000-2017 (d). (unit: in millions of tons) Note: Data for Taiwan, Tibet, Hong Kong and Macau are insufficient

3.3 Coupling relationship between ecological environment quality and carbon emissions

3.3.1 Spatial distribution of CCD values

Fig. 7 showed the coupled coordination degree (CCD) of the ecological environment and carbon emissions and its changes in Chinese counties from 2000 to 2017. The overall coordination level in the eastern region is higher than that in the western region, and the study area has an upward trend. Specifically, counties with slight coordination increased from 570 in 2000 to 911 in 2017, and counties with high coordination increased from 29 in 2000 to 79 in 2017. Spatially, most counties in the Northwest had a low coordination degree (<0.2), which might be attributed to high soil dryness, low vegetation cover, and high surface temperatures in the Northwest. The severe incoordination in the southeastern coastal counties and some counties in the Yangtze River Basin might be due to high carbon emissions, high urbanization, large construction area, and large water body area. Northeastern and central had high coupling coordination degree (>0.6). The 2241 counties (out of 2274 counties) exhibited an increased CCD, and 171 counties displayed a decreased CCD, with an obvious regional difference. The Loess Plateau at the border of Inner Mongolia and Shaanxi Province had the largest increase in local coupling coordination degree (>0.03), indicating that the ecological quality in this region was significantly improved (Fig. 7). The coupling coordination degree in some counties in Xinjiang and the south China was also increased rapidly. Some counties in the Yangtze River Basin, and in some counties in Sichuan, Guangdong, Guangxi, and Yunnan Provinces showed a decreased coupling coordination, which might be related to the decline in ecological quality and the increase in carbon emissions in these places (Fig. 3 and 7).

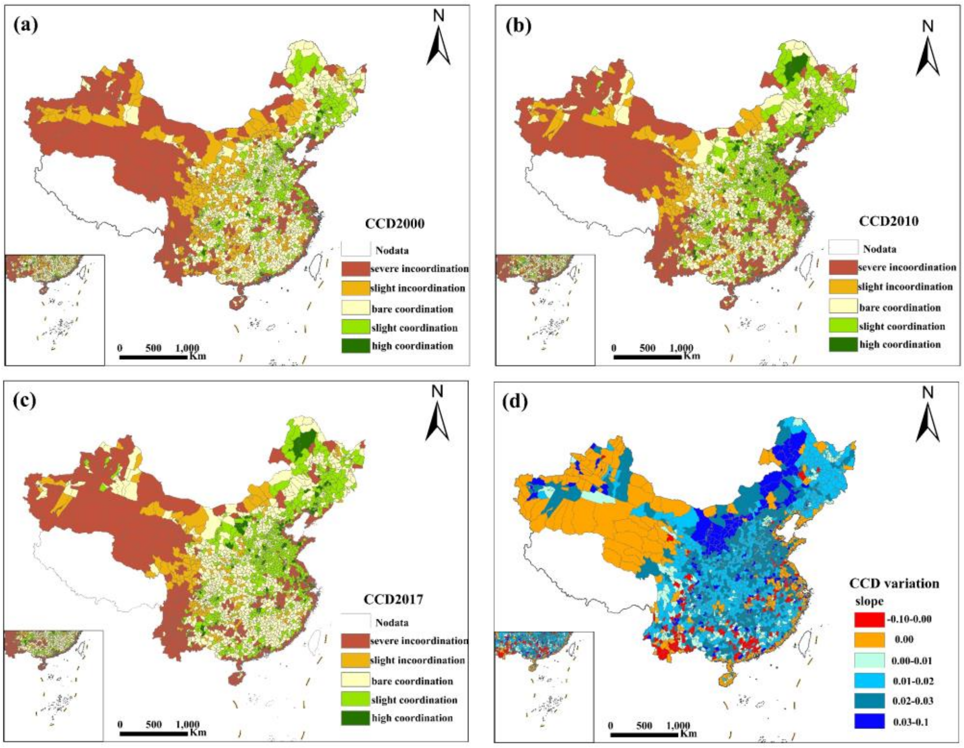

Fig. 7. Spatial distribution of the coupling coordination (CCD values) between energy-related carbon emissions and ecological environment quality in China in 2000 (a), 2010 (b), and 2017 (c) and the change trend from 2000 to 2017 (d).

3.3.2 Spatial clustering characteristics of CCD

In this study, local autocorrelation method was used to study the spatial clustering characteristics of county CCD in 2000, 2010 and 2017. Fig. 8 shows that Moran I value is greater than 0.50 every year, and the dispersion is mainly distributed in the first quadrant and the third quadrant, which shows that the spatial distribution of CCD value has strong clustering, that is, strong clustering. The regions with high/low CCD values tend to cluster. CCD distribution presents a pattern of "low in the west and high in the east". LL-type (low-low) counties are mainly distributed in northwest and southwest China, while HH-type (high-high) counties are mainly distributed in northeast and north China. After 2010, HH-type counties appeared in southern Inner Mongolia. ($P < 0.05$, significance distribution in Fig. 8)

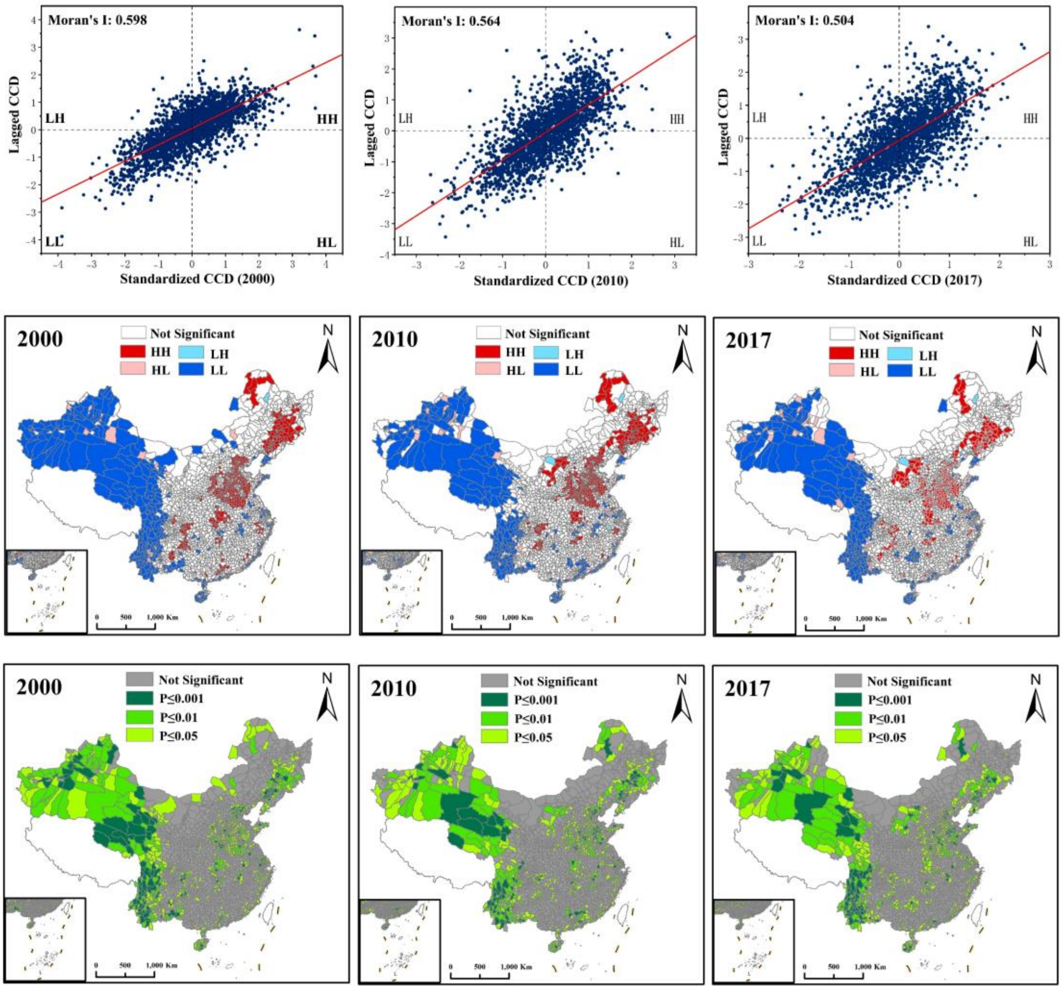

Fig. 8. Local Moran scatter plot (at the top of the figure), local autocorrelation clustering (in the middle of the figure), and significance test (at the bottom of the figure) of CCD distribution for Chinese counties in 2000, 2010, and 2017.

4. Discussion

4.1. Difference between RSEI model and ARSEI model

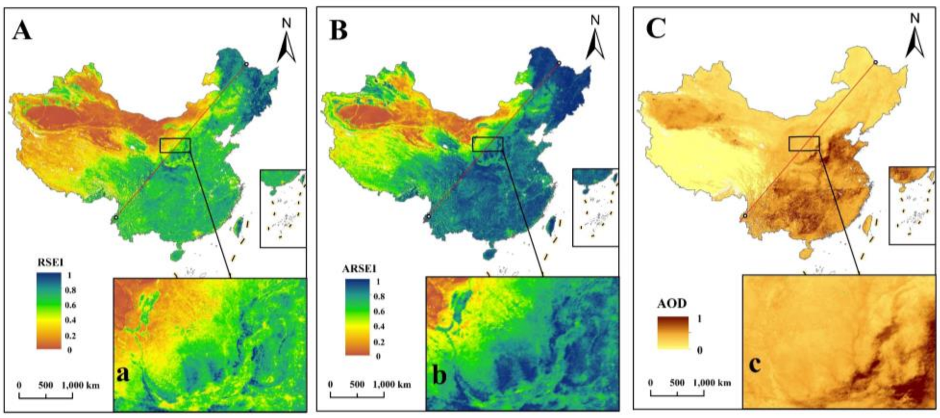

Fig. 9. Distribution of RSEI index (A), ARSEI index (B), and AOD index in 2017 (C).

In recent decades, China's rapid economic development and urbanization have brought about air pollution, which has brought high risks to human health and seriously threatened the coordinated development of the ecosystem (Wu et al., 2018). The RSEI model has been proposed to evaluate ecological environmental quality, but this model neglected the evaluation of air pollution. The previous study has indicated that the RSEI value is lower than the county-level ecological quality index (EQI) value in China obtained during the same period (Xu et al., 2021). Many scholars have utilized AOD to invert the ground particle content (Shin et al., 2020; Wei et al., 2020; Zhang et al., 2020). In the research, the aerosol optical density (AOD) index reflecting the air quality was introduced into the RSEI model to obtain the ARSEI model, which exhibited a stronger adaptability than the RSEI model. Specifically, the ARSEI value was higher than the RSEI value, which was more obvious in the eastern regions (Fig. 9 A and B). In addition, the gap in ecological environment quality between the east and west of the Heihe-Tengchong line was widened, and the gap in ecological environment quality in localized areas was also widened. For example, the gap in ecological environment quality between the north and south of the Tianshan mountain range became bigger. The natural environment in the northern part of the Tianshan Mountains was better than that in the southern part (Wang et al., 2022b), and the AOD value in the southern part of the Tianshan Mountains was higher than that in the northern part (Fig. 9C). The negative correlation between AOD and ARSEI in the ARSEI model resulted in higher ARSEI value in the northern part of the Tianshan Mountains. Therefore, it can be concluded that AOD is mainly responsible for the widened gap in ARSEI values on both sides of the Heihe-Tengchong line and in localized areas.

4.2. Factors influencing spatiotemporal variation of ARSEI

Factors affecting the ecological environment can be categorized into natural and anthropogenic factors (Jiang et al., 2021; Wang et al., 2022a). Natural factors include climate change (Sun et al., 2023), vegetation growth, natural disasters, and others, and anthropogenic factors consist of land use change (Yu et al., 2022a), urbanization (Cai et al., 2021), and ecological restoration projects (Mueller et al., 2014). The causes of ecological environment quality changes vary from region to region.

Our results of ARESI trend analysis indicated that the significant degradation of China’s ecological environment quality mainly occurred in the northern Tianshan mountain range, the northern part of the Greater Khingan Mountains in Northeast China, the Qinghai-Tibet Plateau, the North China Plain, the Yangtze River delta, and some central urban agglomerations. The reasons for the deterioration of the ecological environment are divided into three categories: (1) Poor natural conditions cause ARSEI decline (Zhao et al., 2022). For example, the plateau ecosystem of the Qinghai-Tibetan Plateau is fragile and sensitive to climate change. In the eastern part of this plateau, permafrost is widespread, vegetation is scarce, and thus it is difficult to recover naturally once the ecosystem is damaged (Liang and Song, 2022); (2) The combination of poor natural conditions and human activities leads to a decline in ARSEI. For example, in the northern Tianshan Mountains, the rapid development of inland urban agglomerations with arid climate (Aizizi et al., 2023) consumes a large amount of water resources and interferes with the growth of vegetation (Yu et al., 2023), thus resulting in ecological degradation in the region; (3) Despite good natural conditions, dense population and economic development lead to a decline in ARSEI. For example, with the development of urbanization and industrialization along the southeastern coast and in central China (Yu et al., 2022a; Zhang et al., 2022b), the vegetation has been converted to construction land in large quantities, and the development and consumption of a large number of resources cause air pollution.

The positive influences of climatic and anthropogenic factors on the ecological environment quality cannot be ignored. The reasons for the improvement of the ecological environment fall into two categories. (1) Climate change contributes to ARSEI improvement. For example, the improvements in the ecology of the desert areas of the Tarim Basin and the desert-oasis intertwined zone are mainly due to a warmer and wetter climate (Wang et al., 2022b); the rainfall has increased; and the glacier snowmelt has supplemented the ecological water; (2) Ecological restoration projects have the positive effects on ARSEI improvement. For example, the northeast region in China is affected by the "Three Norths" protection forest (Li et al., 2022) and cropland protection policy (Li et al., 2022). The comprehensive impacts of climate change, extreme weather events and human activities on environmental change need to be further studied. (Hao, 2022).

4.3. Regional coordinated development — Enlightenment from the Loess Plateau

The Loess Plateau is located in the semi-arid area in the north-central part of China, with limited water resources and scarce vegetation, which is a key ecological fragile area. It is worth noting that carbon emissions are increasing in some counties in the northwest of the Loess Plateau (northern Shaanxi, Ningxia, and southern Inner Mongolia), but the ecological environment is improving in this region, but coupling coordination degree is also on the rise. The previous study has pointed out that the ecological risk in the west of Loess Plateau is higher than that in its east (An et al., 2023a), and that the high ecological risk is concentrated in the northwest of this plateau, which is related to the energy and chemical industry and the concentration of industry in this region, and industrial carbon emissions are the dominant sources of carbon emissions in the northwestern counties of the Loess Plateau. At the county level, 20% of the area in typical energy counties concentrates 80% of the carbon emissions (Long et al., 2022), but the hilly and gully regions of these counties have been actively implementing the ecological restoration programs such as "greening at the sacrifice of food production" (Chang et al., 2011), "returning farmland to the forest", and "vegetation restoration" (Song et al., 2022), mine rehabilitation (Bi et al., 2023; Mi et al., 2019), and sediment governance, and these programs have successfully reduced the risk of soil erosion and landslides and enhanced ecosystem carbon sequestration capacity, which are the primary reasons why the Loess Plateau ecosystem has improved and CCD is on the rise. Therefore, the Loess Plateau is a model of coordinated ecological and economic development in arid and fragile areas.

4.4 Coordinated development recommendations

Based on the investigation results of China's ARSEI, carbon emissions, and their coupling coordination degree, we puts forward some suggestions on the harmonious and sustainable development of urban economy and ecology in view of the regional development differences.

In response to the incoordination between the ecological environment and carbon emissions in the west (Xinjiang, Qinghai, Inner Mongolia, Yunnan, and Guizhou provinces), the relevant departments should increase investment in ecological environmental protection and management. Xinjiang is located in an arid zone, whose ecosystems are sensitive to climate change, and ecological restoration policies should focus on climate change and its impact on water resources. Although oasis agriculture improves the ecological environment of desert areas, the high consumption of water resources inhibits its rapid development (Jiang et al., 2021). Anthropogenic factors are the principal factors influencing changes in oasis migration, and the population density and industrial and agricultural production have negative effects on the ecological environment. Therefore, prohibiting the predatory exploitation of water sources, actively implementing water-saving irrigation, constructing protective forest systems (Zhang et al., 2023b), and vigorously developing tertiary industries are effective strategies to promote ecologically sustainable development.

To address the incoordination between the ecological environment and carbon emissions in the east (central urban agglomerations, southwestern regions, coastal cities), the relevant departments should take into account the coordinated management of ecological environment and energy industry. In ecologically fragile areas in Sichuan, Yunnan, and Guizhou provinces, management departments should promote vegetation restoration (Li et al., 2023), reduce soil erosion and landslide risks (Xu et al., 2023), and encourage conservation farming (Jia et al., 2019) and crop rotation management as well as the development of eco-tourism and clean energy industries. In some urban agglomerations with high carbon emissions, measures such as urban greening (Yin et al., 2022), land use layout optimization, and natural water body restoration (such as wetland and urban river restorations) should be taken to improve the microclimate of the urban environment (Finaeva, 2017). Additionally, industrial structure optimization, and low-carbon innovation (Cai et al., 2021), industrialization proportion adjustment, low-consumption high-return renewable resource development should be performed in urban agglomerations (Li et al., 2023b), which is greatly beneficial for urban carbon emission reduction.

5. Conclusion

Based on the GEE platform and remotely sensed data from multiple sources, ARSEI model was constructed to study the temporal and spatial dynamic changes of ecological environment quality in China. In addition, we characterize the spatial and temporal distribution of energy-related carbon (ECE) emissions at the county level in China. Finally, we used the coupling coordination degree model (CCD) to further examine the local coupling coordination relationship between China's ARSEI value and ECE. The results indicate that China's ARSEI has obvious geographic differences, and the Heihe-Tengchong line roughly divides China's ARSEI into two different geographic regions (the East and the West). The east exhibits a higher ARSEI value, with ARSEI in most regions ranging from 0.6 to 1.0, while the west displays a relatively lower ARSEI, with ARSEI in most regions ranging from 0.0 and 0.4. Over the past 22 years, China's regional ecological environment quality has been significantly improved in 24.70% of the area, mainly concentrated in northern and northwestern China. The ecological environment quality in 5.35% of China's area has been significantly degraded, mainly in east China and southwest China. In addition, CCD has a strong spatial aggregation effect, and the distribution of CCD shows a pattern of "west-low-east-high". LL (low-low) -type counties are mainly spread in northwest and southwest China, while HH (high-high)-type counties are mainly located in northeast and north China, and after 2010, HH-type counties appeared in southern Inner Mongolia. The CCD of most counties (2241) exhibited an increasing trend, while that of some counties (171) in southwest China, south China, and central China showed a decreasing trend. Finally, given the low CCD value in western (Xinjiang, Qinghai, Inner Mongolia, Yunnan, Guizhou provinces) and eastern (urban agglomeration, southwest region, coastal cities), we put forward suggestions to promote regional ecological sustainable development and emission reduction according to local conditions.

Funding

This research was supported by the National Key Research and Development Program of China (2021YFD1500703).

Conflict of interest

The authors declare no potential conflict of interest.

References

Aizizi, Y., Kasimu, A., Liang, H.W., Zhang, X.L., Zhao, Y.Y., Wei, B.H., 2023. Evaluation of ecological space and ecological quality changes in urban agglomeration on the northern slope of the Tianshan Mountains. Ecol Indic 146.

An, M., Xie, P., He, W.J., Wang, B., Huang, J., Khanal, R., 2023a. Local and tele-coupling development between carbon emission and ecologic environment quality. J Clean Prod 394.

An, W.K., Wang, B., Duan, L., Giovanni, C., Yu, G., 2023b. Emerging contaminants in the northwest area of the Tai Lake Basin, China: Spatial autocorrelation analysis for source apportionment and wastewater- based epidemiological analysis. Sci Total Environ 865.

Bi, Y.L., Li, M.C., Du, X.P., Christie, P., 2023. Soil aggregation and aggregate-associated organic carbon flows are affected by different restoration patterns on reclaimed mine soil in the Loess Plateau of China. Land Degrad Dev.

Cai, J., Li, X.P., Liu, L.J., Chen, Y.Z., Wang, X.W., Lu, S.H., 2021. Coupling and coordinated development of new urbanization and agro-ecological environment in China. Sci Total Environ 776.

Chang, R.Y., Fu, B.J., Liu, G.H., Liu, S.G., 2011. Soil Carbon Sequestration Potential for "Grain for Green" Project in Loess Plateau, China. Environ Manage 48, 1158-1172.

Chen, J.D., Gao, M., Cheng, S.L., Hou, W.X., Song, M.L., Liu, X., Liu, Y., Shan, Y.L., 2020a. County-level CO2 emissions and sequestration in China during 1997-2017. Sci Data 7.

Chen, J.D., Li, Z.W., Dong, Y.Z., Song, M.L., Shahbaz, M., Xie, Q.J., 2020b. Coupling coordination between carbon emissions and the eco-environment in China. J Clean Prod 276.

Custer, G.F., Dini-Andreote, F., 2022. Embracing Complexity in Ecosystem Response to Global Change. Environ Sci Technol.

Fan, C., Gui, F., Wang, L.Z., Zhao, S., 2020. Evaluation of Environmental Quality Based on Remote Sensing Data in the Coastal Lands of Eastern China. J Coastal Res 36, 1229-1236.

Fan, Y.P., Fang, C.L., Zhang, Q., 2019. Coupling coordinated development between social economy and ecological environment in Chinese provincial capital cities-assessment and policy implications. J Clean Prod 229, 289-298.

Finaeva, O., 2017. Role of Green Spaces in Favorable Microclimate Creating in Urban Environment (Exemplified by Italian Cities). Iop Conf Ser-Mat Sci 262.

Getis, A., Ord, J.K., 1992. The Analysis of Spatial Association by Use of Distance Statistics. Geogr Anal 24, 189-206.

Hao, Z.C., 2022. Compound events and associated impacts in China. Iscience 25.
He, J.Q., Wang, S.J., Liu, Y.Y., Ma, H.T., Liu, Q.Q., 2017. Examining the relationship between urbanization and the eco-environment using a coupling analysis: Case study of Shanghai, China. Ecol Indic 77, 185-193.
Hu, X.S., Xu, H.Q., 2018. A new remote sensing index for assessing the spatial heterogeneity in urban ecological quality: A case from Fuzhou City, China. Ecol Indic 89, 11-21.
Huang, L., Zheng, Y.H., Xiao, T., 2018. Regional differentiation of ecological conservation and its zonal suitability at the county level in China. J Geogr Sci 28, 46-58.
IEA, 2021. An energy sector roadmap to carbon neutrality in China. IEA, Paris.
Jia, L.Z., Zhao, W.W., Zhai, R.J., Liu, Y., Kang, M.M., Zhang, X., 2019. Regional differences in the soil and water conservation efficiency of conservation tillage in China. Catena 175, 18-26.
Jiang, L.G., Liu, Y., Wu, S., Yang, C., 2021. Analyzing ecological environment change and associated driving factors in China based on NDVI time series data. Ecol Indic 129.
Jin, W.Q., Shi, Y.S., 2022. Dynamic Monitoring of Ecological Environment Quality in Gansu Province Supported by Google Earth Engine. Int Arch Photogramm 43-B3, 887-892.
Le Quere, C., Andrew, R.M., Friedlingstein, P., Sitch, S., Pongratz, J., Manning, A.C., Korsbakken, J.I., Peters, G.P., Canadell, J.G., Jackson, R.B., Boden, T.A., Tans, P.P., Andrews, O.D., Arora, V.K., Bakker, D.C.E., Barbero, L., Becker, M., Betts, R.A., Bopp, L., Chevallier, F., Chini, L.P., Ciais, P., Cosca, C.E., Cross, J., Currie, K., Gasser, T., Harris, I., Hauck, J., Haverd, V., Houghton, R.A., Hunt, C.W., Hurtt, G., Ilyina, T., Jain, A.K., Kato, E., Kautz, M., Keeling, R.F., Goldewijk, K.K., Kortzinger, A., Landschutzer, P., Lefevre, N., Lenton, A., Lienert, S., Lima, I., Lombardozzi, D., Metzl, N., Millero, F., Monteiro, P.M.S., Munro, D.R., Nabel, J.E.M.S., Nakaoka, S., Nojiri, Y., Padin, X.A., Peregon, A., Pfeil, B., Pierrot, D., Poulter, B., Rehder, G., Reimer, J., Rodenbeck, C., Schwinger, J., Seferian, R., Skjelvan, I., Stocker, B.D., Tian, H.Q., Tilbrook, B., Tubiello, F.N., van der Laan-Luijkx, I.T., van der Werf, G.R., van Heuven, S., Viovy, N., Vuichard, N., Walker, A.P., Watson, A.J., Wiltshire, A.J., Zaehle, S., Zhu, D., 2018. Global Carbon Budget 2017. Earth Syst Sci Data 10, 405-448.
Lenzen, M., Malik, A., Foran, B., 2016. Reply to Schandl et al., 2016, JCLEPRO and Hatfield-Dodds et al., 2015, Nature: How challenging is decoupling for Australia? Reply to: Schandl H., Hatfield-Dodds S., Wiedmann T., Geschke A., Cai Y., West J., Newth D., Baynes T., Lenzen M. and Owen A. (2016). Decoupling global environmental pressure and economic growth: scenarios for energy use, materials use and carbon emissions. Journal of Cleaner Production 132: 45-56; Hatfield-Dodds S., H. Schandl, PD Adams, TM Baynes, TS Brinsmead, BA Bryan, FH Chiew, PW Graham, M. Grundy, and T. Harwood. (2015). Australia is 'free to choose' economic growth and falling environmental pressures. Nature 527(7576): 49-53. J Clean Prod 139, 796-798.
Li, T., Bao, R., Li, L., Tang, M.F., Deng, H.B., 2023. Temporal and Spatial Changes of Habitat Quality and Their Potential Driving Factors in Southwest China. Land-Basel 12.
Li, Z.D., Wang, S., Li, C.J., Ye, C.C., Gao, D.X., Chen, P., 2022. The trend shift caused by ecological restoration accelerates the vegetation greening of China's drylands since the 1980s. Environ Res Lett 17.
Liang, Y., Song, W., 2022. Integrating potential ecosystem services losses into ecological risk assessment of land use changes: A case study on the Qinghai-Tibet Plateau. J Environ Manage 318.
Liu, P., Ren, C.Y., Yu, W.S., Ren, H.X., Xia, C.Z., 2023. Exploring the ecological quality and its drivers based on annual remote sensing ecological index and multisource data in Northeast China. Ecol Indic 154.
Liu, Q., Yu, F.H., Mu, X.M., 2022. Evaluation of the Ecological Environment Quality of the Kuye River Source Basin Using the Remote Sensing Ecological Index. Int J Env Res Pub He 19.
Liu, Y.Y., Yang, Y., Wang, Q., Du, X.L., Li, J.L., Gang, C.C., Zhou, W., Wang, Z.Q., 2019. Evaluating the responses of net primary productivity and carbon use efficiency of global grassland to climate variability along an aridity gradient. Sci Total Environ 652, 671-682.
Long, Y., Jiang, F.G., Deng, M.L., Wang, T.H., Sun, H., 2023. Spatial-temporal changes and driving factors of eco-environmental quality in the Three-North region of China. J Arid Land 15, 231-252.
Long, Z., Sun, Y., Lang, L., Chen, X., Zhang, Z., Pang, J., 2022. Characteristics and spatial-temporal pattern of carbon emissions in typical counties of the Loess Plateau: A case study of Qingcheng County. Arid zone research 39, 1631-1641.
Lv, Q., Liu, H.B., Yang, D.Y., Liu, H., 2019. Effects of urbanization on freight transport carbon emissions in China: Common characteristics and regional disparity. J Clean Prod 211, 481-489.
Mi, J.X., Liu, R., Zhang, S.L., Hou, H.P., Yang, Y.J., Chen, F.Y., Zhang, L.M., 2019. Vegetation patterns on a landslide after five years of natural restoration in the Loess Plateau mining area in China. Ecol Eng 136, 46-54.

Mueller, T., Dressler, G., Tucker, C.J., Pinzon, J.E., Leimgruber, P., Dubayah, R.O., Hurtt, G.C., Bohning-Gaese, K., Fagan, W.F., 2014. Human Land-Use Practices Lead to Global Long-Term Increases in Photosynthetic Capacity. Remote Sens-Basel 6, 5717-5731.
Shin, M., Kang, Y., Park, S., Im, J., Yoo, C., Quackenbush, L.J., 2020. Estimating ground-level particulate matter concentrations using satellite-based data: a review. Gisci Remote Sens 57, 174-189.
Song, W.Q., Feng, Y.H., Wang, Z.H., 2022. Ecological restoration programs dominate vegetation greening in China. Sci Total Environ 848.
Sun, T., Yang, Y.M., Wang, Z.G., Yong, Z.W., Xiong, J.N., Ma, G.L., Li, J., Liu, A., 2023. Spatiotemporal variation of ecological environment quality and extreme climate drivers on the Qinghai-Tibetan Plateau. J Mt Sci-Engl 20, 2282-2297.
Tang, F., Wang, L., Guo, Y.Q., Fu, M.C., Huang, N., Duan, W.S., Luo, M., Zhang, J.J., Li, W., Song, W., 2022. Spatio-temporal variation and coupling coordination relationship between urbanisation and habitat quality in the Grand Canal, China. Land Use Policy 117.
Tang, Q., Hua, L., Cao, Y.F., Jiang, L., Cai, C.F., 2023. Human activities are the key driver of water erosion changes in northeastern China. Land Degrad Dev.
Teng, F., 2015. Resolve ambiguities in China's emissions. Nature 525, 455-455.
Wang, J.B., Ding, Y.F., Wang, S.Q., Watson, A.E., He, H.L., Ye, H., Ouyang, X.H., Li, Y.N.A., 2022a. Pixel-scale historical-baseline-based ecological quality: Measuring impacts from climate change and human activities from 2000 to 2018 in China. J Environ Manage 313.
Wang, J.J., Ding, J.L., Ge, X.Y., Qin, S.F., Zhang, Z., 2022b. Assessment of ecological quality in Northwest China (2000-2020) using the Google Earth Engine platform: Climate factors and land use/land cover contribute to ecological quality. J Arid Land 14, 1196-1211.
Wang, Z.B., Liang, L.W., Sun, Z., Wang, X.M., 2019. Spatiotemporal differentiation and the factors influencing urbanization and ecological environment synergistic effects within the Beijing-Tianjin-Hebei urban agglomeration. J Environ Manage 243, 227-239.
Wei, X.L., Chang, N.B., Bai, K.X., Gao, W., 2020. Satellite remote sensing of aerosol optical depth: advances, challenges, and perspectives. Crit Rev Env Sci Tec 50, 1640-1725.
Wise, M., Calvin, K., Thomson, A., Clarke, L., Bond-Lamberty, B., Sands, R., Smith, S.J., Janetos, A., Edmonds, J., 2009. Implications of Limiting CO2 Concentrations for Land Use and Energy. Science 324, 1183-1186.
Wu, X.G., Ding, Y.Y., Zhou, S.B., Tan, Y., 2018. Temporal characteristic and source analysis of PM2.5 in the most polluted city agglomeration of China. Atmos Pollut Res 9, 1221-1230.
Xin, J.Y., Ma, Y.J., Zhao, D.D., Gong, C.S., Ren, X.B., Tang, G.Q., Xia, X.A., Wang, Z.F., Cao, J.J., de Arellano, J.V.G., Martin, S.T., 2023. The feedback effects of aerosols from different sources on the urban boundary layer in Beijing China. Environ Pollut 325.
Xiong, Y., Xu, W.H., Lu, N., Huang, S.D., Wu, C., Wang, L.G., Dai, F., Kou, W.L., 2021. Assessment of spatial?temporal changes of ecological environment quality based on RSEI and GEE: A case study in Erhai Lake Basin, Yunnan province, China. Ecol Indic 125.
Xu, D., Yang, F., Yu, Y., Zhou, Y.Y., Li, H.X., Ma, J.J., Huang, J.C., Wei, J., Xu, Y., Zhang, C., Cheng, J., 2021. Quantization of the coupling mechanism between eco-environmental quality and urbanization from multisource remote sensing data. J Clean Prod 321.
Xu, X.J., Yan, Y.J., Dai, Q.H., Yi, X.S., Hu, Z.Y., Cen, L.P., 2023. Spatial and temporal dynamics of rainfall erosivity in the karst region of southwest China: Interannual and seasonal changes. Catena 221.
Xu, Y.M., Shen, Y., 2013. Reconstruction of the land surface temperature time series using harmonic analysis. Comput Geosci-Uk 61, 126-132.
Yang, H.H., Yu, J., Xu, W.Z., Wu, Y., Lei, X.Y., Ye, J.N., Geng, J.W., Ding, Z., 2023. Long-time series ecological environment quality monitoring and cause analysis in the Dianchi Lake Basin, China. Ecol Indic 148.
Yang, Y.S., Ni, C.J., Jiang, M.J., Chen, Q.Y., 2021. Effects of aerosols on the atmospheric boundary layer temperature inversion over the Sichuan Basin, China. Atmos Environ 262.
Yang, Z.J., Sun, C., Ye, J.W., Gan, C.Y., Li, Y., Wang, L.Y., Chen, Y.J., 2022. Spatio-Temporal Heterogeneity of Ecological Quality in Hangzhou Greater Bay Area (HGBA) of China and Response to Land Use and Cover Change. Remote Sens-Basel 14.
Ye, H., 2022. Analysis on Ecological Environment Change of Kalajun-Kurdening World Natural Heritage Site from 2006 to 2019. Pol J Environ Stud 31, 915-927.
Yu, G.T., Liu, T.W., Wang, Q., Li, T., Li, X.J., Song, G.H., Feng, Y.G., 2022a. Impact of Land Use/Land Cover Change on Ecological Quality during Urbanization in the Lower Yellow River Basin: A Case Study of Jinan City. Remote Sens-Basel 14.

Yu, J.B., Li, X.H., Guan, X.B., Shen, H.F., 2022b. A remote sensing assessment index for urban ecological livability and its application. Geo-Spat Inf Sci.

Yu, T.T., Abulizi, A., Xu, Z.L., Jiang, J., Akbar, A., Ou, B., Xu, F.J., 2023. Evolution of environmental quality and its response to human disturbances of the urban agglomeration in the northern slope of the Tianshan Mountains. Ecol Indic 153.

Zhang, J., Yang, L., Gong, E., Wang, Y., Ren, J., Liu, M., 2023a. Dynamic monitoring of ecological environment quality in Xi'an based on Google Earth cueing and improved remote sensing ecological index. Journal of Ecology 43, 2114-2127.

Zhang, J., Zhang, P., Gu, X.C., Deng, M.J., Lai, X.Y., Long, A.H., Deng, X.Y., 2023b. Analysis of Spatio-Temporal Pattern Changes and Driving Forces of Xinjiang Plain Oases Based on Geodetector. Land-Basel 12.

Zhang, M.M., Kafy, A.A., Ren, B., Zhang, Y.W., Tan, S.K., Li, J.X., 2022a. Application of the Optimal Parameter Geographic Detector Model in the Identification of Influencing Factors of Ecological Quality in Guangzhou, China. Land-Basel 11.

Zhang, X.Y., Wang, F., Wang, W.H., Huang, F.X., Chen, B.L., Gao, L., Wang, S.P., Yan, H.H., Ye, H.H., Si, F.Q., Hong, J., Li, X.Y., Cao, Q., Che, H.Z., Li, Z.Q., 2020. The development and application of satellite remote sensing for atmospheric compositions in China. Atmos Res 245.

Zhang, Y., She, J.Y., Long, X.R., Zhang, M., 2022b. Spatio-temporal evolution and driving factors of eco-environmental quality based on RSEI in Chang-Zhu-Tan metropolitan circle, central China. Ecol Indic 144.

Zhao, Z.Y., Li, T., Zhang, Y.L., Lu, D., Wang, C., Lu, Y.H., Wu, X., 2022. Spatiotemporal Patterns and Driving Factors of Ecological Vulnerability on the Qinghai-Tibet Plateau Based on the Google Earth Engine. Remote Sens-Basel 14.